Hindawi
Shock and Vibration
Volume 2023, Article ID 7152223, 18 pages
https://doi.org/10.1155/2023/7152223

Research Article

A Dynamic Design Methodology for Large-Scale Complex Nonlinear Systems Based on Orthogonal Decomposition Technique

Qi-Bin Wang,[1] **Si-Yang Piao**,[1] **Ming-Wei Piao**,[2] **Peng Dang**,[3] **Qiu-Ze Li**,[3] **and Jing-Ying Ren**[1]

[1]*College of Locomotive and Rolling Stock Engineering, Dalian Jiaotong University, Dalian, Liaoning 116028, China*
[2]*Mech. Eng. School, Dalian Jiaotong University, Dalian, Liaoning 116028, China*
[3]*CRRC Changchun Railway Vehicle Co. Ltd., Changchun, Jilin 130062, China*

Correspondence should be addressed to Ming-Wei Piao; m_w_piao@126.com

Received 21 August 2022; Revised 18 December 2022; Accepted 19 December 2022; Published 10 January 2023

Academic Editor: Junhong Park

HSRS is taken as a typical research case of large-scale complex nonlinear systems, and the re-innovation of associated imported technologies needs to be combined with the particularities of Chinese HSR practices, seeking a more suitable dynamic design methodology to conduct the self-adaptive improved design. Different from the troublesomeness of the primary hunting phenomenon, the self-adaptive improved design can decrease considerably the impact of car body instability on ride comfort merely by applying the semiactive damping technique between intervehicles, to promote scientifically the limit and construction speeds under the rational conditions of wheel-rail matching, i.e., $\lambda_{eN} \geq \lambda_{\text{emin}}$, $\lambda_{\text{emin}} = (0.03\text{–}0.05)$. The researching viewpoint of hunting kinematics makes the investigations on the geometric nonlinearity of the wheel-rail contacts contrary to the hypothesis of small creepage and no spin. Since the technical prototype of German ICE3 serial bogies has the design default of the primary hunting phenomenon, the improved design of the wheel-rail relationship has simply abandoned the high-quality technical resources of wheel-rail matching conditions at low conicity. On the contrary, the dynamic simulation analyses of MC01-TC02-MC03 three-vehicles trainset show that the semiactive damping technique between intervehicles takes advantage of $I_{zz} >> I_{xx}$ to improve the impacts of car body instability on ride comfort, and the self-adaptive improved design has consequently the ability to achieve the technical goal of uniform wear at low conicity. On the premise of meeting the requirements of crossing over different speed grade dedicated lines and realizing the running operations on three-speed levels of 160/250/350 km/h, the self-adaptive higher-/high-speed bogies can conditionally satisfy the economic reprofiling requirements of wheelsets through the optimal routing planning.

1. Introduction

The application of a large number of analysis software is one of the main technical characteristics in postindustrial societies. Nevertheless, large-scale complex nonlinear systems such as high-speed rolling stock (HSRS) must also rely on big data mining techniques such as orthogonal decomposition or modal modification so as to carry out the dynamic design. The optimal configuration of higher-/high-speed bogies can be guided instructively with the analysis graphs of full vehicle stability properties and variation patterns, realizing the goal of scientifically promoting the limit and construction speeds under rational conditions of wheel-rail matching at the minimum cost. Therefore, the HSRS operation and maintenance practice for High-Speed Rails (HSR) has become an incredible engineering in postindustrial societies, which actively boosts the formation and development of dynamic design methodology.

Uniform wear at low conicity should be one of the necessary technical conditions for worldwide HSR practices. The commercial application vision of future HSR transport is necessary to be clarified in the planning for HSR

construction, so as to achieve the three technical goals of low conicity, low power dissipation, and low dynamic interaction, and to expand investment profits by high-speed freight rails. Similar to conventional rail transportation, the HSR commercial application also needs to maintain the hunting motion stabilization as much as possible in order to achieve the above three technical goals. Slightly different from the development plan of Chinese HSR construction, the second-stage planning for pan-European HSR construction was disclosed recently [1], which includes the following three main points: (a) an investment of ca. 10.5 billion Euros will be used for the speeding up and upgrading of existing rail lines and the construction of new planned lines of ca. 2×10^4 km; (b) special emphasis was placed on the construction of economic corridors among regional centers, and the longest traveling time by high-speed train was extended to ca. 5 hours; and (c) the valuable experiences are fully affirmed gained from the trial operations of freight train Sgnss with speeding up to 160 km/h on German ICE (InterCity Express) rails and the ETR500 freight trainset with 200 km/h running on Italian rail lines, and the potential demand is also defined for the future Eurasian transcontinental HSR construction with the capacity of 600 t per freight train on HSR.

However, wheel-rail contact has a dialectical relationship between (near-) linearity and nonlinearity. From the experimental studies on lateral stability done by Matsudaira [2] to Wickens' worn stability theory [3–5], the research on the geometric nonlinearity of wheel-rail contact completely breaks the assumption of small creepage and no spin, i.e., the hunting motion stabilization is conditional. Specifically, the geometric nonlinearity of wheel-rail contact forces the wheel to produce spin creepage and then form a rolling resistance moment. Therefore, the longitudinal traction kinetic energy is partially transformed into the lateral one of instability-hunting oscillation.

Wheel-rail contact has then the duality of hunting kinematics and dynamics. Accordingly, UIC518 or EN14363 and other specifications clearly put forward the following two contradictory technical provisions: (a) when $v > 280$ km/h, the actual equivalent conicity λ_e shall not be greater than 0.15, to maintain the hunting motion stabilization as much as possible; (b) once the instability hunting oscillation occurs accidentally, the bogie vibration early warning mechanism must be enforced. At present, the safety threshold is determined by the empirical formula, which only depends on the mass of the whole bogie, including the front and rear wheelsets. Thus, it can be seen that the geometric nonlinearity of wheel-rail contact will force the steady state of hunting movement to change, no matter normal wear or detrimental wear.

Chinese HSR practices cannot absolutely place the expectation of theoretical and methodological innovations on some analysis software. Similar to the wheel-tire self-stabilization of road vehicles, Schiehlen insists that [6] hunting motion stabilization is unconditional. Accordingly, some analysis software blindly implements the undifferentiated processing method of rail and road vehicle MBS (Multi-Body System) and carries out the so-called distributed multidisciplinary collaborative simulations with the invariant step integration algorithm of Space State Reduction (SSR). The quasistatic perturbation simulation based on hunting kinematics makes the rail vehicle MBS completely overlook the two important nonlinear factors of wheel-rail contact and bogie suspension.

The improved design of the high-speed wheel-rail relationship tries to maintain the contact relationship of (near-) linearity at a very high cost. The first ETR 600 tilting train launched by ALSTOM after the acquisition of the tilting technique from FIAT had switched to traditional antiyaw dampers. By virtue of preventive and maintenance rail grinding treatments with modified profiling of the railhead, it attempts to meet the speed requirement of 300 km/h under the track conicity condition of $(\mathrm{RMS})_{3\sigma} \leq 0.05$ with an occurrence probability of 99.75% for the service lines in mountainous regions [7]. However, similar to the wear law of Japanese Shinkansen rails, ETR 600 only transfers the work of reducing wear and dissipation to the rail discipline.

As far as the technical prototype of Japanese Shinkansen bogies is concerned, the vertical coupling resonance occurs accidentally in the equipment cabin under the floor, e.g., the traction converters, which are the behaviors in unsaturated or unsteady states caused by the mutual influences of two different nonlinear vibrations. Although the surface hardness of wheel tread is moderately increased, too many times of wheelset reprofiling under the floor may cause dynamic imbalance problems, which force the front and rear bogies to oscillate towards each other or back [8–10].

By using the variable step integration algorithm with three-stage of forecast correction evaluations, the literature [11] fully proved that the above technical prototype has the occurrence probability of longitudinal and vertical coupling resonance. The associated vibration reduction problem makes the general DVA (Dynamic Vibration Absorber) lose its application premise, i.e., narrowband response characteristics [12]. In order to avoid the vertical coupling resonance of the traction converter, the mono-rod traction device reduces the traction stiffness per bogie by improving the design of rubber joints at both ends of the link between the car body and front/rear bogies, which is counterproductive and increasing the occurrence probability of longitudinal and vertical coupling resonance.

Such improvement can only make the axle load of an empty vehicle exceed the limit seriously due to the repeated structural reinforcement designs. If the application research neglects the use conditions of existing techniques, the results will only become worse and worse, and there will even be a more unrealistic idea of imposing multiple DVAs [13, 14].

As far as the practices of German ICE rails are concerned, the rail grinding treatment is not a successful experience at all. In particular, the primary hunting default of ICE3 serial prototype bogies [15], forced the operation and maintenance of German ICE Rails into the technical traps of passenger dedicated line or special vehicle dedicated line.

Under the configuration of novel antiyaw dampers, i.e., ZF Sachs T60/T70 with the working principle of mono-/dual-circulation, the implementation of rail grinding has not achieved the expected goal of uniform wear at low conicity.

The actual equivalent conicity λ_e shows [7] that there is a rapid linear increasing trend within the operating mileage of more than 20×10^4 km; then, the saturation value λ_e is represented with a large degree of dispersion, and the wear stabilization at high conicity is maintained with the average values of ca. 0.25/0.20 for motor/trailer vehicles, respectively. Considering the two-point contact near to wheel flange root, the Rolling Radius Difference (RRD) curve forms a negative slope change near the zero-crossing point. At the cost of RCF (rolling contact fatigue) failure on the rail shoulder at one side of the rail gauge corner, the reprofiling period of the wheelset can reach $(35–45) \times 10^4$ km. It can be seen above that the rail grinding only plays a positive role in delaying the RCF failures on the rail shoulders at one side of the gauge corner.

Since the back-to-back distance of the wheelset is 1360 mm for speeding up on European existing rails or Japanese Shinkansen rails, the kinetic energy of the instability hunting oscillation is attenuated by the friction heat consumption. However, the technical prototype of CRH3C is German ICE3 serial bogies, and the renewal design of the wheel profile with thin flange has replaced the original S1002G (flange thickening 3.5 mm, or referred to as S1002CN) when wheelset reprofiling under the floor [16]. Since the wheel-rail clearance on each side increases by 3.5 mm, $\lambda_e = (0.17–0.18)$, the dynamic behavior of the CRH3C trainset becomes very serious after the first wheelset reprofiling under the floor. Even after the second wheelset reprofiling under the floor, the actual running mileage can only reach ca. 10×10^4 km due to the dynamic interaction impacts caused by central hollow tread wear.

Considering the long-term operation of high-speed grade dedicated lines, $\lambda_e \geq 0.10$, the proportion of tangent running or curving negotiation with a large radius is relatively high in routing, and the central hollow tread wear has become one of the technical bottlenecks in Chinese HSR practices. Even today, such as CR400BF, the actual equivalent conicity increases rapidly and linearly in the running mileage of less than 20×10^4 km from (0.10–0.12) at the new car state or after the wheelset reprofiling under the floor, but when it approaches (0.30–0.35), the car body fluttering phenomenon that occurs accidentally becomes more and more severe. The actual RRD curve forms a discontinuous change near the zero-crossing point [17], and the research on the geometric nonlinearity of wheel-rail contact is contrary to the assumption of small creepage and no spin. Considering the change in wheel spin singularity, the local conformal or bad contact that occurs now and then on the railhead of some specific sections due to worn wheel-rail contact geometry, the frequency of instability hunting oscillations can even reach (7.0–8.0) Hz or higher.

For the increasingly severe dynamic impacts of worn wheel-rail contact, Polach no longer adheres to his viewpoint of small amplitude hunting safety, but proposes instead his updated design of the wheel profile [18], expanding the light bandwidth of tread contact to reduce the negative impacts caused by the nonlinear geometry of wheel-rail contact. However, considering the detrimental tread wear or flange wear caused by high-speed wheelsets [7, 8, 17], Polach has also to admit [19] that the determination of wheel-rail contact geometric parameters cannot ignore the response output of rail vehicle systems, e.g., car body shaking phenomenon, which will produce the associated negative impacts feedback to wheel creepage and wear.

Except for the parallel combination of four ZF Sachs T70 dampers per bogie for long formation trains [20], the central hollow tread wear has been extended at present to all HSRS with novel antiyaw dampers like ZF Sachs T60, which causes the (shallow-) surface faults on wheel tread and railhead, or bogie vibration alarm, or more and more serious car body fluttering phenomenon [21, 22]. The vibration comfort is then decreased rapidly in the middle floor, e.g., the lateral and vertical comfort indexes W_z reaches or exceeds 4.0. In addition, the coupling resonance of the diamond mode in the middle of the service car body is becoming more and more intense, which will expose the defects of the roof structure, such as the crescent notch and transverse weld seam near the pantograph fairing. Therefore, central hollow tread wear is becoming one of the unsafe factors affecting high-speed wheel-rail contact.

The antirolling torsion bar devices have the occurrence probability of complex constraint singularity changes, which form the correlation relationship with car body shaking phenomenon, thereby giving up simply the high-quality resources and losing the rational condition of wheel-rail matching, i.e., $\lambda_e < 0.10$ [15]. Since bridges and tunnels account for more than 90% of some mountain rail lines, considering the open and dark lines staggered, the cross-wind, side wind, or wake disturbances on the service car body will inevitably have negative impacts on the corresponding wheel creepage and wear through antirolling torsion bar devices. Thus, it can be seen that considering the back-to-back distance of the wheelset is shortened to 1353 mm and the wheel-rail clearance on each side has then increased by 3.5 mm, the negative impacts of the above feedback will cause the fluctuations of wheel spin singularity, which force the wheel tread to produce the problem of lateral uneven power dissipation when long-term speeding up on a dedicated line with $\lambda_e \geq 0.10$.

More than ten years of Chinese HSR practices have fully proved that the central hollow tread wear and associated negative impacts cannot be eliminated merely by the improved design of the high-speed wheel-rail relationship. Moreover, considering that it is difficult to control the rail grinding error between individual dedicated lines, the technical feasibility of crossing operation over different dedicated lines is then decreasing constantly [23], and the central hollow tread wear is also difficult to be self-cleaned.

In particular, CRH5 (including the antiwind/sand trainset) has also experienced car body shaking when the servicing speed is increased to 250 km/h on high-speed grade dedicated lines [24]. Considering the constant speed hypothesis, the falling-off accident of the long transmission shaft may occur again. Similarly, the CRH1 model manufactured by BST (Bombardier Sifang (Qingdao) Transportation Ltd.) has been canceled.

To remove and eliminate the detrimental wear and associated negative impacts is one of the technical bottlenecks in

worldwide HSR practices. Especially the operating mileage of Chinese rails has reached 15.5×10^4 km at present, including HSR of 4.2×10^4 km, accounting for 27.1%. Therefore, the commercial applications of HSR must have key techniques to improve the associated technical economy. There are two technical solutions to detrimental wear as follows: one is the improved design of the wheel-rail relationship of HSR [25], as stated above; the other is the self-adaptive improved design of higher-/high-speed bogies, making it become a technical platform for MDO (Multidiscipline Design Optimization) among vehicles, rails, and passenger transport.

The rational condition of wheel-rail matching is one of the necessary conditions for the implementation of a uniform wear strategy at low conicity in worldwide HSR practices. The rail discipline unilaterally improves the design of the wheel-rail relationship for HSR, and the present methods include rail grinding, wheelset reprofiling under the floor, renewal design of wheel profile, and brake grinding on the wheel tread. If there is no return to the rational conditions of wheel-rail matching, the above methods can not completely fix the problem of detrimental wear, nor can they completely eliminate the phenomenon of service car body fluttering.

Different from conventional rails, HSRS is the main body of the HSR transport system; e.g., there are two design solutions for 160 km/h bogies: one is not configured with antiyaw dampers, and the other is equipped with antiyaw dampers, which depends on the conditions of wheel-rail matching for the servicing lines. However, as far as the HSR transport system is concerned, only when HSRS is scientifically speeded up under the rational conditions of wheel-rail matching can the technical economy of commercial applications be improved so as to expand the income on investment with high-speed freight rails.

As a classic large-scale complex nonlinear system, the high-speed trainset has three kinds of nonlinear vibrations of forced, parametric, and self-excited. These nonlinear vibrations interact with each other mainly due to the change of complex constraint singularity. To this end, our research proposes a dynamic design methodology, including the following three key techniques as follows:

(a) The self-adaptive improvement direction of higher-/high-speed bogies is defined by using the analysis graph of full-vehicle stability properties and variation patterns and big data mining techniques such as orthogonal decomposition or modal modification, i.e., the nominal equivalent conicity $\lambda_{eN} \geq \lambda_{\text{emin}}$, the minimum allowable value $\lambda_{\text{emin}} = (0.03–0.05)$

(b) By using the rigid-flex coupling simulation technique, the Finite Element Model (FEM) modification technique based on the load-type processing on component interfaces is used to further improve the transacting strategy of the flexible car body to MBS interface, and the inherent rigid-flex coupling relationship of the HSRS system is then reasonably constructed

(c) By applying the three-stage variable step integration algorithm for forecast, correction, evaluation proposed by Negrut, and the correctness of Modal Stress Recovery (MSR) is ensured by the precise analysis results of complex constrained inner forces [19, 20], thus realizing the seamless integration with Dong's structural stress recovery and weld fatigue damage assessment methods

In order to expand the ICE transportation revenue, the German DB Rail Company adopts the trainsets Sgnss of articulated container flatcars to carry out the express freight rail transportation. Taking the freight frame bogie Y25 as the front/rear end bogies and middle articulated bogie, literature [26] has formulated a new countermeasure to reduce wear and dissipation. Specifically, for the curve negotiation with a radius of 375 m, the best combination of tread wear and flange wear can be obtained through the optimization of track parameters such as outer rail superelevation, gauge, and bottom inclination, and the technical goal of reducing wear and dissipation is then achieved.

Inspired by the above creative measures to reduce wear and dissipation, this research has finished the following two previous works [27, 28], i.e., the two self-adaptive improved solutions for higher-/high-speed bogies and the weak coupling design to ensure a 30-year service life of a car body made of aluminum alloy.

Based on the above previous works, this paper takes the self-adaptive high-speed bogie with the parallel configuration of four ZF Sachs T60 dampers as the research object. Firstly, the HSRS dynamic design methodology is briefly discussed when considering the main nonlinear factors in Section 2; the parameter sensitivity analysis is carried out to clarify the car body instability problem to be solved in Section 3; the dynamic simulation analysis of a three-vehicle trainset is conducted to verify the semiactive damping technique between intervehicles in Section 4; finally, the technical advantages of self-adaptive high-speed trainsets are demonstrated through contrastive analyses of typical cases in Section 5; and conclusions and prospects are summarized in Section 6.

2. HSRS Dynamic Design Methodology

As for large-scale complex nonlinear systems such as HSRS, the dynamic design methodology is a serial method of system design based on the precise analysis results of complex constrained inner forces, in which the analysis graphs of full-vehicle stability properties and variation patterns are key technology.

2.1. Duality of Hunting Kinematics and Dynamics. Wickens thinks that Japanese Shinkansen practices have not solved the worn stability problem; details can be seen in [29]. For this purpose, Chinese HSR practices of HSRS operations and maintenance should inherit and carry forward the scientific spirit of Wickens presented in establishing his worn stability theory, i.e., the duality of hunting kinematics and dynamics, seen in [3–5].

Under the assumption of small creepage and no spin, when $\lambda_e < 0.10$, the steady state with constant speed, the following wheel-rail lateral dynamic equilibrium relationship can be proved in the following equation:

$$(\delta_e W)y \approx (2f_\eta)\psi. \tag{1}$$

in the equation, δ_e is the equivalent linear parameter of a contact angle difference, W is the axle load of the wheelset, and f_η is the coefficient of longitudinal creepage defined for the lateral and yaw movements of the wheelset.

The left side of equation (1) is the feedback response of the restoring force formed by the gravity stiffness due to the lateral displacement y of the wheelset, while the right side is the lateral component of the longitudinal creeping force caused by the yaw angle ψ of the wheelset. Thus, the wheel-rail lateral dynamic equilibrium relationship is constituted, which is consistent with Schiehlen's viewpoint.

The wheelset hunting is composed of associated lateral and yaw harmonic motions, i.e. $y(t) = y_0 \sin(\omega t), \psi(t) = \psi_0 \cos(\omega t)$. If the condition as shown in equation (2) is satisfied, i.e., $\psi_0 \longrightarrow 0$, we can then get Klingel's formula as shown in equation (3).

$$\begin{aligned} &\frac{\psi_0}{y_0} = \frac{\omega}{v}\ (\psi_0 \to 0) \\ &\quad \text{or} \\ &\frac{\psi_0}{y_0} = \frac{\omega}{v}, \psi_0 \to 0, \end{aligned} \tag{2}$$

$$\lambda_e = \left(\frac{2\pi}{L}\right)^2 e_0 r_0. \tag{3}$$

According to the second-order differential equation as shown in equation (4), the wheel-rail contact geometry, such as actual RRD (rolling radius difference) curve $\Delta r(y)$, determines the curvature $1/\rho$ variation as shown in equation (5) of the hunting motion trajectory.

$$\frac{d^2 y}{dx^2} + \frac{\Delta r(y)}{2r_0 e_0} = 0, \tag{4}$$

$$-\frac{d^2 y}{dx^2} \approx \frac{1}{\rho} \propto \Delta r(y), \tag{5}$$

where in y_0 and ψ_0 are the amplitudes of wheelset lateral and yaw motions, respectively; v is the rolling speed of the wheelset; ω is the circular frequency of wheelset hunting motion; L is the hunting motion wavelength of the wheelset, $f = \omega/2\pi = v/L$, ca. (1.0–2.0) Hz; e_0 is half of the lateral span of the nominal rolling circles; r_0 is the radius of the nominal rolling circle; and x is the travel coordinates of wheelset along the hunting motion trajectory.

But with the increasing speed, if $\lambda_e \geq 0.10$, there is then

$$(\delta W)y \neq F(\gamma), \tag{6}$$

tin which, $F(\gamma)$ is the lateral creeping force generated by wheel spin γ. Considering that the frequency of the instability hunting oscillation is increased, the lateral inertial force of the wheelset breaks the above equilibrium relationship, thus forming the fluctuation of the wheel spin singularity, $\gamma > 0.6$, which makes the wheel slip instantaneously.

Under the premise of small creepage and no spin assumption, Kalker proposed a FastSim simplified program. When FastSim was first applied to the wheel-rail contact nonlinear element, the high spin correction [5] was adopted to better maintain the wheel-rail lateral dynamic equilibrium, as shown in equation (6).

Wickens completely proposed the research problem of nonconservative systems with constrained wheelsets [3, 4]. Specifically, the radial forced steering bogies to have the remaining problem of High Creepage Issue under the rigid constraints of wheelset positioning, which requires the introduction of wheel spin to explain the geometric nonlinear impacts to the lateral uneven power dissipation on the tread.

The large-scale complex nonlinear system such as rail vehicles has two kinds of nonlinear influences, i.e., nonsmoothness, and large displacement, and has three classes of nonlinear vibrations, i.e., forced, parametric, and self-excited. For a class of nonsmooth nonlinear problems, True strongly opposes the use of a constant step integration algorithm [30], which makes it difficult to grasp exactly the changes and influences of complex constraint singularities.

As far as the large displacement nonlinear problem is concerned, i.e., holonomic and nonholonomic constraints constitute complex constraints, and the corresponding Jacobian matrix may be ill-conditioned accidentally, the improved variable step integration algorithm proposed by Negrut has become one of the effective research means to promote the rapid development of modern rail vehicle system dynamics [31–33]. Specifically, according to the principle of the virtual work, the improved generalized augmentation method accurately captures the minimum resistance perturbation direction by using the ingenious combination of generalized independent variables and virtual augmented variables, forming a variable step integration algorithm with a three-stages of the forecast, correction, and evaluation. Therefore, the rail vehicle system no longer meets the principles of modal orthogonality and (anti-) symmetry of modal shapes [34].

In general, the wheel-rail contact has a dialectical relationship between (near-) linearity and nonlinearity, which mainly depends on the influences of wheel spin singularities caused by geometric nonlinearity. Just as light has wave-particle duality, so the wheel-rail relationship of HSR also has the duality of hunting kinematics and dynamics.

2.2. Five Particularities of Chinese HSR Practices. The re-innovation of imported technologies of HSRS should not be separated from the following five particularities of Chinese HSR practices:

(1) Considering the back-to-back distance of the wheelset, $L_0 = 1353$ mm, the wheel-rail clearance on each side for Chinese HSR is 3.5 mm larger than that of existing European rails or Japanese Shinkansen rails. Thus, only when $\lambda_e < 0.10$, can the low wear area of wheel-rail contact become wider, forming a uniform wear stage at low conicity, and meeting the assumption of small creepage and no spin. Therefore, this high-quality resource for wheel-rail matching

cannot be easily abandoned only due to the design default of the primary hunting phenomenon that existed in the technical prototype of CRH3 bogies.

(2) Because of $\lambda_e \geq 0.10$, the long-term operations of speeding up on dedicated lines and the actual routing with the unreasonable ratio of curvature to straightness, the central hollow tread wear has then become an exclusive event with a high probability, and there is almost no flange root wear or flange side wear. The geometric nonlinearity of wheel-rail contact forces the wheels to produce spin creepage and form a rolling resistance moment, which gradually changes the hunting motion stabilization into the instability hunting oscillation with a small amplitude. As a result, the associated wheels have lateral uneven power dissipation on tread, such as the characteristics of both ends cocked in the wear index distribution.

(3) The proportion of bridges and tunnels on some mountain lines can reach more than 90%. Since the open and dark lines are staggered, the crosswind, sidewind, and wake disturbance force the service car body to roll and rock, resulting in a fluid-solid coupling effect, which enhances the negative impact feedback to associated wheel creepage and wear. On some specific rail sections, the local conformal or bad contact is formed between the central hollow worn tread and the railhead top, which makes the mutual influences occur accidentally between the parametric and self-excited nonlinear vibrations, i.e., unsaturated or nonsteady behaviors.

(4) As the maximum starting acceleration of the EMU (Electric Multiple Units) can reach 0.05 g, the influence of severe regional climate conditions such as across the Nanling Mountains has to be considered on the traction coefficient. Once wheels slip instantaneously, scrapes or blotches may become flat scars. Some scholars believe that flat scars are one of the main inducements for the formation of longitudinal uneven wear in wheel-rail rolling.

(5) Considering that the rubber pad under the rail is the only damping element of the ballastless track bed, and the wheelset dynamic imbalance impacts caused by some wheels with flat scars may make the local seamless rail produce the ca. 540 Hz lateral coupling resonance, which poses a very serious challenge to the fatigue safety of key components or the pretightening and antiloosening measures for various types of bolts in the running gear system. Similarly, the dynamic imbalance problems will also be caused due to too many times of wheelset reprofiling under the floor.

2.3. Three Main Achievements in Chinese HSRS Transformation

2.3.1. Longitudinal and Vertical Coupling Resonance. Compared with Japanese Shinkansen practices, bogie articulation and car body tilting are two key technologies for speeding up on existing European rails, but rail grinding is the precondition for their successful applications. Specifically, under the specific service line conditions with the track conicity $(\mathrm{RMS})_{3\sigma} \leq 0.05$ with an occurrence probability of 99.75%, traditional antiyaw dampers are used for ETR 600 serial bogies, so as to implement the overdamped mechanism to restrain hunting motion and achieve the technical goal of uniform wear at low conicity.

Instead of the two-point contact on the rail shoulder at one side of the gauge corner, as shown in Figures 1(a)–1(c), the two-point contact on the railhead top has become one of the unique manifestations of detrimental wear in Chinese HSR practices.

For the speeding up on existing European rails, when the standard wheel S1002 is matched to UIC rail E1 with a bottom inclination of 1/20, the back-to-back distance of the wheelset is 1360 mm, $\lambda_{eN} \approx 0.01$, and the initial contact point on the railhead is inclined to one side of the field and there is ca. 10 mm distance from the centerline of the railhead. In the low-wear area, the contact points of the left and right wheel treads are basically unchanged to maintain the near-linearity relationship between wheel-rail contacts.

Relatively speaking, as the back-to-back distance of the wheelset is shortened to 1353 mm, the wheel-rail clearance on each side of Chinese HSR has increased by 3.5 mm. When the LMA tread is matched to the rail CN60KG (equivalent to UIC rail E2 with a bottom inclination of 1/40), $\lambda_{eN} \approx 0.03$, the low wear area is moderately expanded. However, the change of the actual RRD curve is still one of the main constraints limiting the amplitude of wheelset hunting motions.

The wear survey of long-term speeding-up operations on dedicated lines shows that the actual RRD curve will have a discontinuous change near to zero-crossing point when the mileage is less than 5×10^4 km [8]. For this reason, some wheelsets have to undergo frequent reprofiling under the floor; thus, forming a technical and economic problem for CRH2C speeding up to 300 km/h. In particular, the installation of hanging frame cracks of traction converters is caused by the longitudinal and vertical coupling resonance. As mentioned above, the DVA is hard to work because of the vertical resonance caused by the mutual influences of two different nonlinear vibrations, i.e., unsaturated or unsteady state behaviors.

2.3.2. Negative Feedback Impacts of Car Body Roll and Rock. As far as Chinese HSR practices are concerned, the technical transformation of CRH5 (including anticold trainsets and wind-/sand-proof trainsets) has better explained the rational condition of wheel-rail matching.

XP55 tread is one of the technical achievements formed by the mutual transformation of the above two different track parameters, which has been successfully applied in the HSR practices for both CRH in China and KTX in South Korea. Similarly, as the back-to-back distance of the wheelset, $L_0 = 1353$ mm, when the XP55 tread is matched to the rail CN60KG with a bottom inclination of 1/40, $\lambda_{eN} \approx 0.06$, the corresponding low wear area is also significantly expanded. As far as the CRH5 bogie is concerned, as shown in Figure 1(d), which is one of the

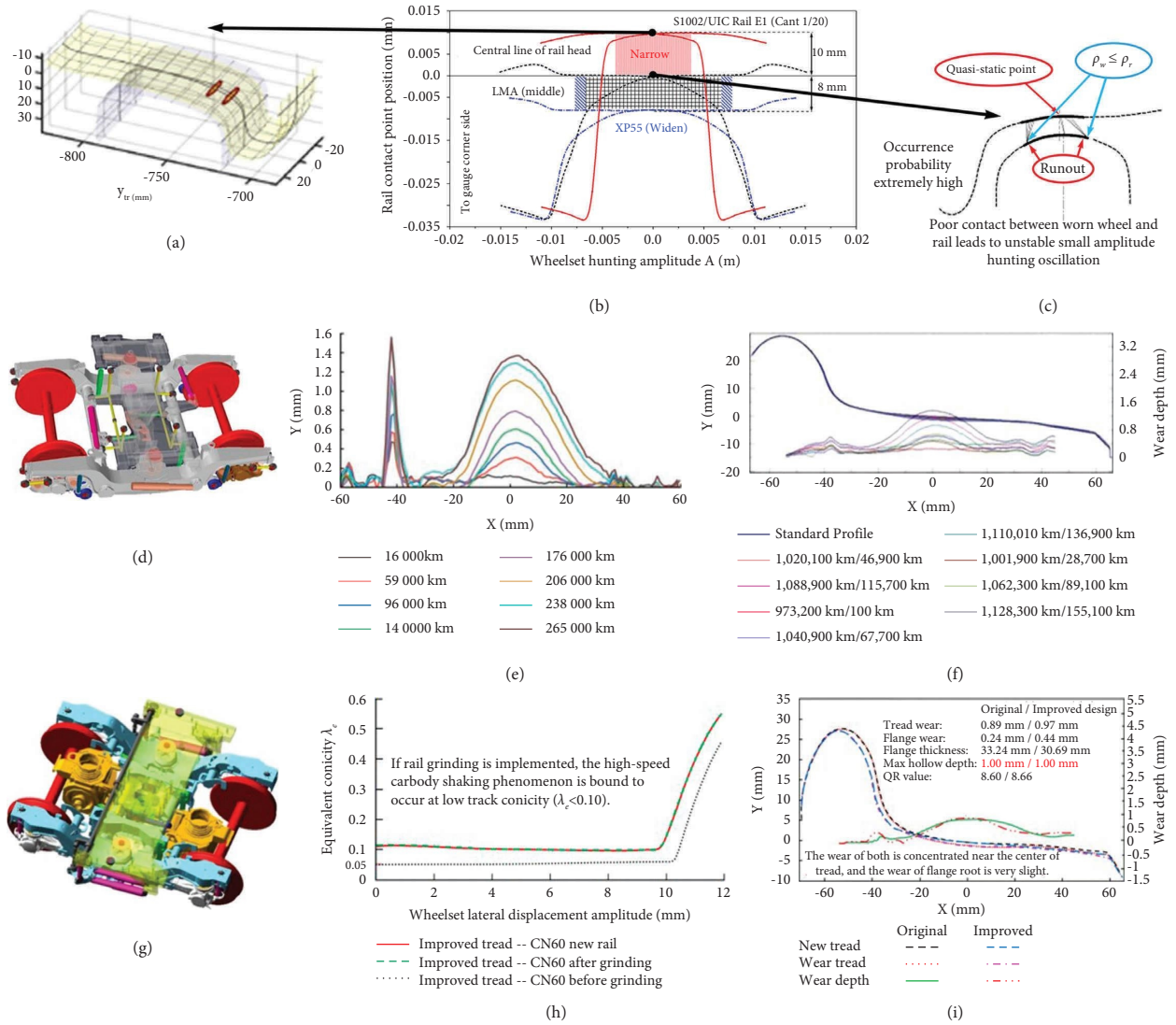

Figure 1: Influences of track parameters on the low-wear area of wheel-rail contact and detrimental wear evolution such as central hollow tread wear in Chinese HSR practices. (a) Two-point contact problem on the rail shoulder at one side of the gauge corner. (b) Comparison of three typical wheel-rail matching. (c) Two-point contact problem on rail top with stronger dynamic interaction. (d) Template model of a CRH5 bogie with an antirolling torsion bar device with dual bars per bogie. (e) Tracking measuring results on wheel wear when CRH5 trainset in 200 km/h running. (f) Wear characteristics of central hollow tread wear after CRH5 speeding up to 250 km/h on an HSR dedicated line. (g) Template model of an ICE3 motor bogie for high-speed rails. (h) Equivalent conicity curve contrast for wheel profile renewal design LMB-10 to rail CN60KG before or after grinding. (i) Tread wear comparison for wheel profile original and renewal designs.

improved design forms of ETR serial tilting bogies, the compound bolster is removed with the tilting mechanism, and the air-spring suspension is used instead of steel spring ones, but the antirolling torsion bar device is retained with the dual torsion bars per bogie. The ratio of curvature to straightness is rational in actual routing when running across the 200 km/h grade dedicated lines and ordinary speed rails. As shown in Figure 1(e), there is an equilibrium between tread and flange wear, by which the longest mileage can reach ca. 30×10^4 km for wheelset reprofiling. Therefore, the wheel-rail matching conversion from S1002 to XP55 tread has proved successful in Chinese HSR practices of 200 km/h operation and maintenance.

However, the CRH5 is experiencing a very serious car body shaking phenomenon when the long-term operation of speeding up to 250 km/h on dedicated lines, as shown in Figure 1(f), and the central hollow tread wear is one of the main reasons for the above phenomenon. Considering that the traction motors are suspended under the floor, the long transmission shafts may fall off again. The car body shaking phenomenon will cause the lateral coupling resonance of traction motors and associated hanging frames, the dominant frequency of which is ca. 7.0 Hz. According to the constant speed condition of the transmission shaft, the whole transmission system will also have torsional resonance, which forces the universal joints at both ends to fail.

2.3.3. Rational Condition of Wheel-Rail Matching. As far as the CRH3C bogies are concerned, with four ZF Sachs T60 configurations per bogie, as shown in Figures 1(g)–1(i), the central hollow tread wear is formed eventually no matter the rail grinding treatment or the wheel profile renewal design, which is mainly manifested in the following three aspects: (1) high-speed shaking phenomenon at low conicity of $\lambda_e < 0.10$ after rail grinding [21]; (2) central hollow tread wear is eventually formed in long-term operations on dedicated lines with $\lambda_e \geq 0.10$ [17, 20]; and (3) the service car body fluttering phenomenon may occur accidentally and become more and more serious when $\lambda_e \approx (0.30–0.35)$ [22, 28].

So, how should we give a reasonable explanation for the formation mechanism of the above detrimental wear? In particular, when the wheel-rail clearance is increased by 3.5 mm on each side of the Chinese HSR, no matter what causes the car body to roll and rock, it will force the associated wheels to have a negative impact feedback on their creepage and wear, thus enhancing the response output of the service car body when $\lambda_e < 0.10$, which leads to the vibration comfort problems, i.e., high speed shaking phenomenon. This high-quality technical resource of wheel-rail matching was thereby easily abandoned. At the same time, the long-term speeding-up operations on dedicated lines with $\lambda_e \geq 0.10$ force the wheels to produce gradually the spin creepage, which results in lateral uneven power dissipation on the tread. The wheel-rail local conformal contact or poor contact makes the associated wheelsets form instability-hunting oscillations with small amplitude, thus forming a disturbance source causing the bogie vibration early warning or car body fluttering phenomenon.

2.4. Full-Vehicle Stability Properties and Variation Patterns. Because the dynamics of the HSRS system have two classes of nonlinear influences caused by nonsmoothness and large displacement, as stated above, it is necessary to use the improved algorithm of variable step integration to obtain the precise analysis results of complex constrained inner forces under the support of a better hardware and software platform. Nevertheless, the calculation complexity and low efficiency force this large-scale complex nonlinear system impossible to carry out the MDO.

The MDO based on Pareto includes such elements as a nondominant solution, clustering division, and key minority. The application of orthogonal decomposition or modal modification techniques can reasonably execute clustering division and better face the frontier of Pareto design [35]. Esp. under the condition of multiple constraints, the MDO such as the HSRS system should adopt a dialectical and unified analysis viewpoint [36], i.e., the hunting motion stabilization is conditional, which depends on the geometric nonlinearity of worn wheel-rail contact.

Compared with the conventional root locus graph, the analysis graph of full-vehicle stability properties and variation patterns purposed in this research has three important features, i.e., closed-loop pole, stability margin (or critical damping), and convected motion relationship. The convected motion relationship refers to the convected motion formed between relevant modes caused by the complex constraint singularity in the generalized space, which constitutes the corresponding kinetic or potential energy exchange or transformation.

And the convected motion relationship depends on the ill-conditioned number of the Jacobian matrix [37, 38]. For this reason, the analysis graph of full-vehicle stability properties and variation patterns is the best tool for optimal parameter configuration of higher-/high-speed bogies, eliminating the unfavourable convected motion relationship and making the beneficial one more robust.

2.5. Design Default of Primary Hunting Phenomenon. As a design default of German ICE3 serial bogies, the discovery and demonstration of the primary hunting phenomenon formation mechanism should become one of the most important achievements in the CRH3C/380BL technology transformation. Under the antiyaw dampers ZF Sachs T60/T70 (mono-/dual-circulation) configuration, the analysis graphs of motor-vehicle stability properties and variation patterns are shown in Figures 2(a) and 2(b), both of which are corresponding, respectively, to the operation situations of the Köln to Frankfurt section in German ICE rails and the Madrid to Barcelona section in Spain AVE (Alta Velocidad Española) rails with wide gauge 1674 mm.

To increase unilaterally the critical velocity, the ICE3 serial bogies adopt the strong rigid constraints of wheelset positioning, i.e., longitudinal/lateral stiffness is, respectively, 120/12.5 MN/m. However, the car body yaw modes are almost over-damped, so that the yaw phase margin of the rear bogie is then forced to be decreased rapidly. Consequently, the primary hunting phenomenon occurs between rear bogie hunting mode and car body rolling mode. For $\lambda_e < 0.10$, the car body shaking phenomenon will occur at high-speed running with vibration comfort problems. Nonetheless, this high-quality technical resource for $\lambda_e < 0.10$ cannot be simply abandoned. Although the vibration comfort problem has been partially solved, the rail grinding treatment implemented in German ICE rails did not yet achieve the expected effectiveness of uniform wear at lower track conicity.

For the motor vehicle under the configurations of an imported serial bogies ICE3, the generalized mass of instability hunting oscillations can be reduced effectively by the convected motion relationship between the hunting modes of the motor bogies and the lateral swaying ones of corresponding traction motor hangers. Furthermore, unlike the simple problem of car body instability, the primary hunting phenomenon is a troublesome technical problem, which refers that the car body yaw over-damped characteristics force the yaw phase margin of the rear bogie to decline rapidly, which makes the unfavourable convected motion relationship to be established with the car body rolling mode. The antiroll torsion bar devices are improperly used due to the primary hunting phenomenon, which forces the wheel tread to have central hollow tread wear in Chinese practices of HSR dedicated lines [39, 40].

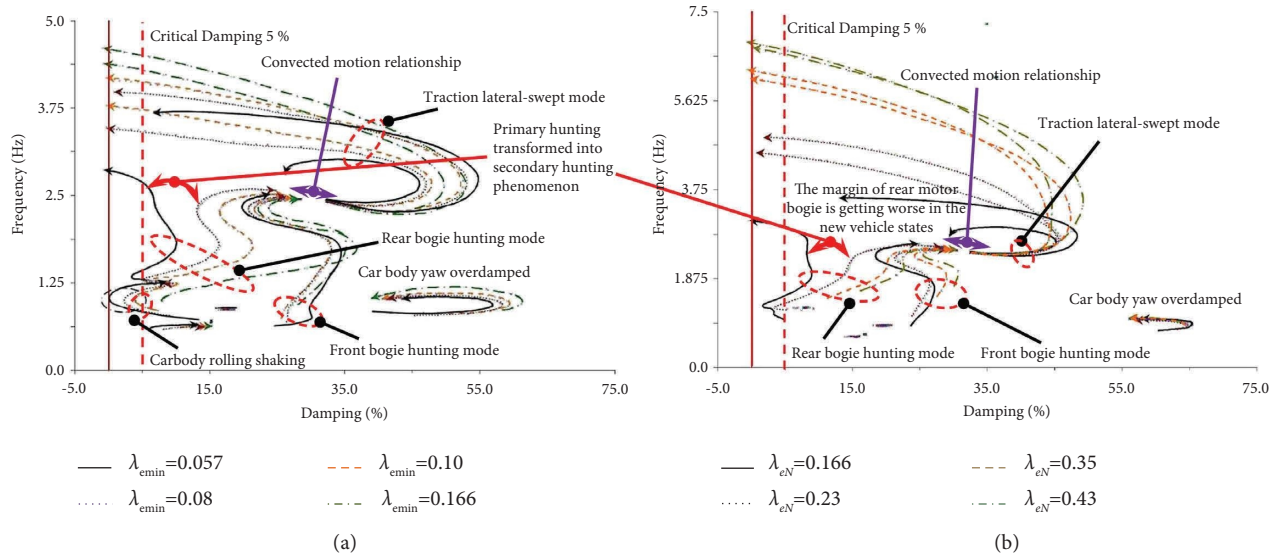

Figure 2: Primary hunting phenomenon occurred in German ICE3 serial bogies with ZF Sachs T60/T70 configurations. (a) Under ZF Sachs T60 original configuration with end-joint stiffness 70 MN/m. (b) Under ZF Sachs T70, the improved configuration with end-joint stiffness of 25 MN/m.

In summary, from the analysis viewpoint on the technology and economy of commercial HSR applications, it is impossible to copy foreign experience to solve our difficult problem of central hollow tread wear, such as the improved design of wheel-rail relationship of Chinese HSR with the present means of rail grinding, wheelset reprofiling under the floor, renewal design of wheel profile, and tread brake grinding. Aiming at large-scale complex nonlinear systems, such as HSRS and associated characteristics, this research proposes the dynamic design methodology, which uses the variable step integration algorithm to ensure the precise analysis of complex constrained inner forces and applies the analysis graph of full-vehicle stability properties and variation patterns to clarify the self-adaptive improved direction of higher-/high-speed bogies. Therefore, Chinese HSR practices are making contributions to better solving the remaining problems of the High Creepage Issue, e.g., the self-adaptive improved designs for higher-/high-speed bogies.

3. Self-Adaptive High-Speed Bogies and Car Body Instability Problem

The Mark 4 passenger train of UK rails always has a very serious wheel wear problem [7]. Starting from the relationship between the rational RRD curve of the wheelset and the lateral even power dissipation on tread [41], literature [42] proposed the following solution, i.e., incorporating hydraulic damping in the bogie primary suspension, such as a hydraulic joint of axle box rotating arm with the higher technical risk. As mentioned above, the self-adaptive improved design of a higher-/high-speed bogie should solve the difficult problem of detrimental wear at the minimum cost.

Under the configuration of self-adaptive high-speed bogies, as shown in Figures 3(a)–3(c), the analysis graphs of stability properties and variation patterns for the motor vehicles show as follows:

(a) Compared with the prototype design of German ICE3 serial bogies, the parameter configuration has been modified in the self-adaptive improved design, e.g., the longitudinal/lateral stiffness of wheelset positioning has been reduced from 120/12.5 MN/m per axle box to 15/6 MN/m per axle box, and the lateral/vertical stiffness of the motor hanger rubber joints has been changed to 440 kN/m × 4 per bogie. The original design adopts the leaf spring suspension, and the swept laterally stiffness is only 110 kN/m × 4 per bogie.

(b) ZF Sachs T60 is still selected as the redundant design, i.e., four novel antiyaw dampers per bogie, but the parameters of which are adjusted as follows: hydraulic stiffness is decreased to 3 MN/m, and the rating value of linear damping is increased to 480 kN·s/m, and the linear rating value of secondary lateral dampers is increased to 30 kN·s/m.

(c) In order to solve the troublesomeness of the primary hunting phenomenon, the self-adaptive improved design still needs to deal with the problem of car body instability at the minimum cost. Special attention should be paid: different from the car body shaking phenomenon in high-speed running at lower track conicity, as shown in Figures 3(d)–3(f), the problem of car body instability has a correlation to the antirolling torsion bar devices.

When $\lambda_e = 0.05$ and the longitudinal stiffness of wheelset positioning is (14–26) MN/m, the motor vehicle stability properties and variation patterns demonstrate the self-adaptive high-speed improved design has the parameter

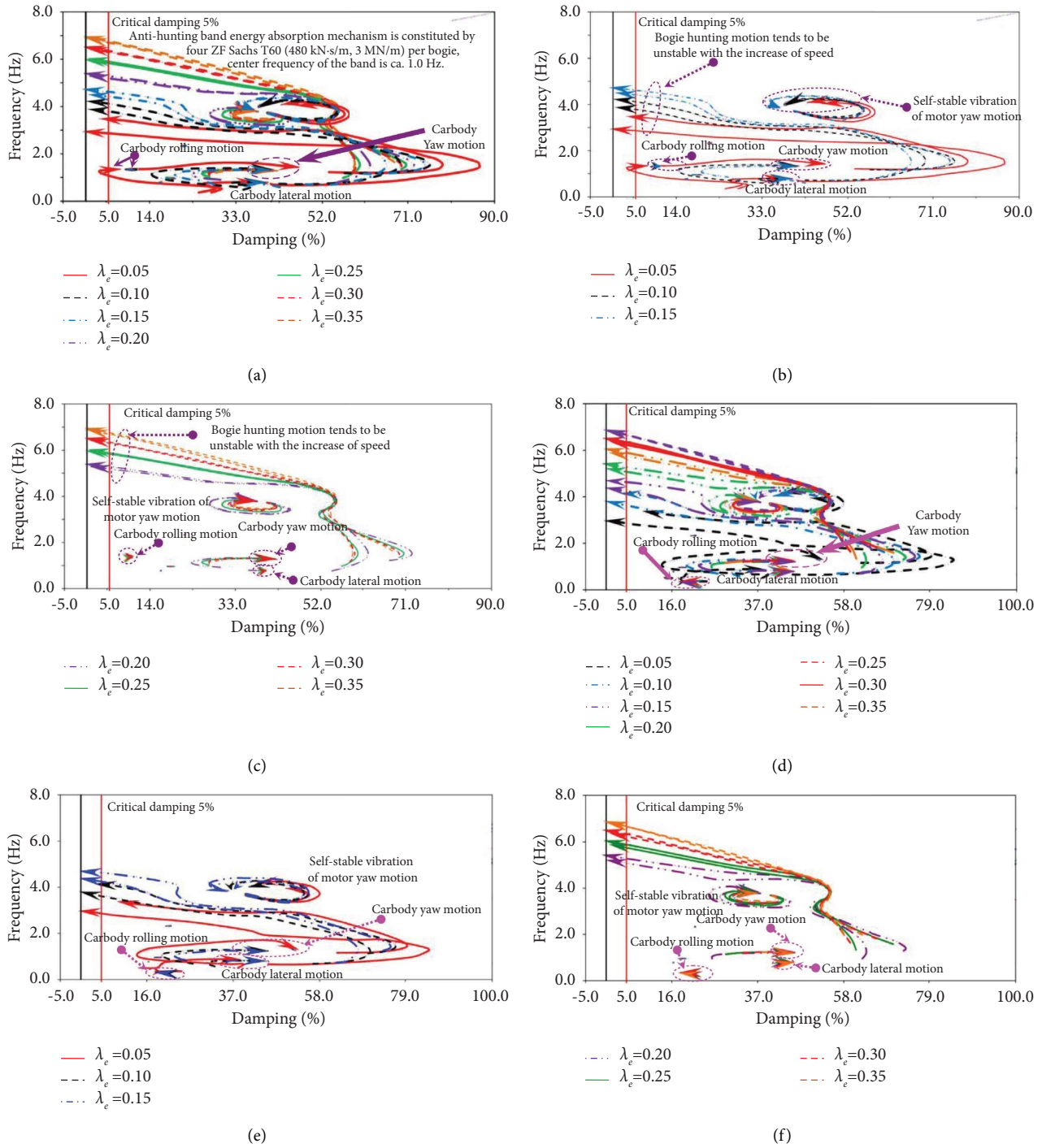

FIGURE 3: Analysis graphs of stability properties and variation patterns for a self-adaptive improved motor vehicle with antirolling torsion bar devices (in-) active. (a) When $\lambda_e = 0.05–0.35$ with antirolling torsion bar devices active. (b) When $\lambda_e = 0.05–0.15$ with antirolling torsion bar devices active. (c) When $\lambda_e = 0.20–0.35$ with antirolling torsion bar devices active. (d) When $\lambda_e = 0.05–0.35$ with antirolling torsion bar devices inactive. (e) When $\lambda_e = 0.05–0.15$ with antirolling torsion bar devices inactive. (f) When $\lambda_e = 0.20–0.35$ with antirolling torsion bar devices inactive.

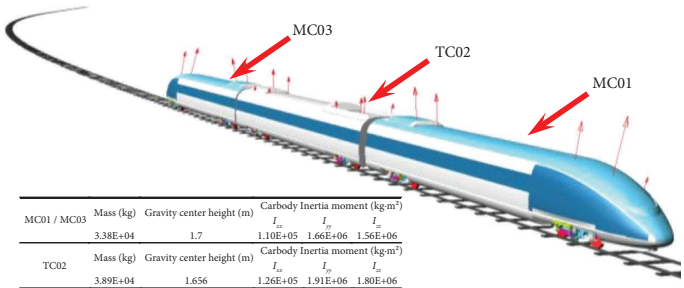

MC01 / MC03	Mass (kg)	Gravity center height (m)	Carbody Inertia moment (kg·m²)		
			I_{xx}	I_{yy}	I_{zz}
	3.38E+04	1.7	1.10E+05	1.66E+06	1.56E+06
TC02	Mass (kg)	Gravity center height (m)	Carbody Inertia moment (kg·m²)		
			I_{xx}	I_{yy}	I_{zz}
	3.89E+04	1.656	1.26E+05	1.91E+06	1.80E+06

(a)

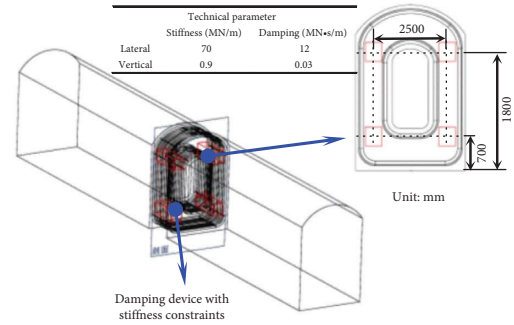

(b)

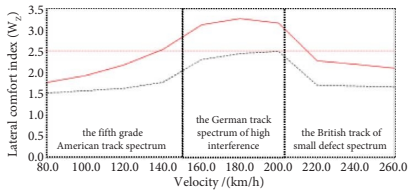

No inter-carbody damping, Maximal lateral W_Z=3.26
Inter-carbody damping, Maximal lateral W_Z=2.49

(c)

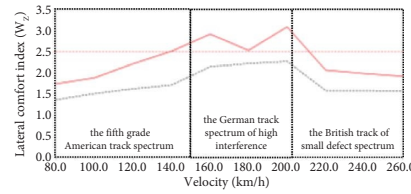

No inter-carbody damping, Maximal lateral W_Z=3.09
Inter-carbody damping, Maximal lateral W_Z=2.28

(d)

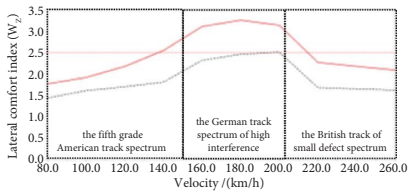

No inter-carbody damping, Maximal lateral W_Z=3.26
Inter-carbody damping, Maximal lateral W_Z=2.51

(e)

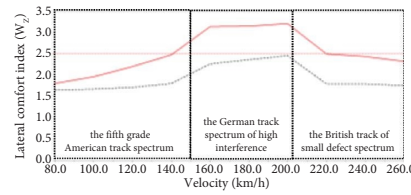

No inter-carbody damping, Maximal lateral W_Z=3.20
Inter-carbody damping, Maximal lateral W_Z=2.45

(f)

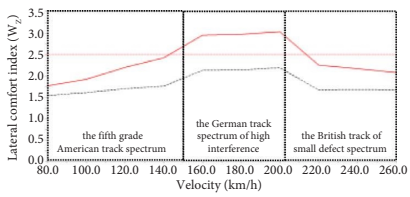

No inter-carbody damping, Maximal lateral W_Z=3.03
Inter-carbody damping, Maximal lateral W_Z=2.19

(g)

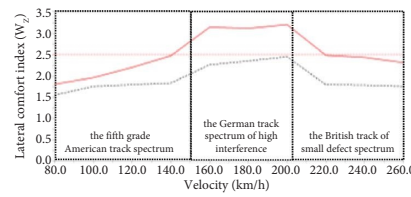

No inter-carbody damping, Maximal lateral W_Z=3.20
Inter-carbody damping, Maximal lateral W_Z=2.45

(h)

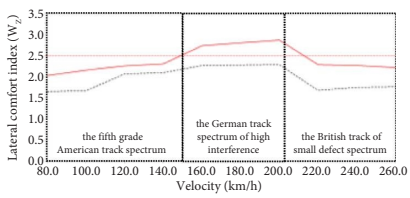

No inter-carbody damping, Maximal lateral W_Z=2.87
Inter-carbody damping, Maximal lateral W_Z=2.26

(i)

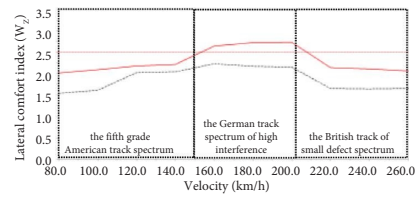

No inter-carbody damping, Maximal lateral W_Z=2.73
Inter-carbody damping, Maximal lateral W_Z=2.23

(j)

Figure 4: Continued.

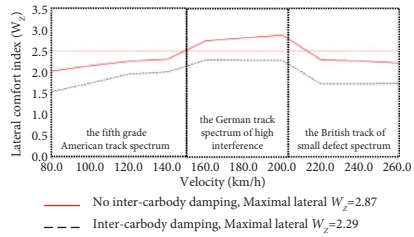

(k)

Figure 4: Three-vehicle trainset with semiactive damping techniques between intervehicles and technical effective assessments. (a) Three-vehicle trainset simulation of motor-trailer-motor in curing negotiation. (b) Semiactive damping device between intervehicles. (c) Lateral comfort index at rear car body MC01 under $\lambda_e = 0.03$. (d) Lateral comfort index at the rear car body TC02 under $\lambda_e = 0.03$. (e) Lateral comfort index at rear car body MC03 under $\lambda_e = 0.03$. (f) Lateral comfort index at rear car body MC01 under $\lambda_e = 0.06$. (g) Lateral comfort index at the rear car body TC02 under $\lambda_e = 0.06$. (h) Lateral comfort index at rear car body MC03 under $\lambda_e = 0.06$. (i) Lateral comfort index at rear car body MC01 under $\lambda_e = 0.10$. (j) Lateral comfort index at the rear car body TC02 under $\lambda_e = 0.10$. (k) Lateral comfort index at rear car body MC03 under $\lambda_e = 0.10$.

insensitive changes. Similarly, for secondary lateral dampers and antiyaw dampers, it can also be demonstrated that the self-adaptive high-speed improved design has also parameter insensitive changes when the rating value of their linear damping changes within a certain range.

In summary, the main technical features of a self-adaptive high-speed bogie are as follows:

(a) A rational matching relationship is formed between the dynamical features of antiyaw dampers and the constraint stiffness of the wheelset positioning so that the over-damped characteristics of car body yaw mode are transformed into the small damped one, and the yaw phase margin of the front and rear bogies becomes then sufficient;

(b) A "spoiler effect" is formed between the front and rear bogie hunting modes and the corresponding motor yaw modes, i.e., the front and rear motors and their hangers oscillate with opposite yaw to restrain the rapid attenuation of the corresponding bogie yaw phase margin. But when $\lambda_e = 0.25/0.30/0.35$, the "spoiler effect" suppresses the fast attenuation of the front and rear bogie yaw phase margins. Notwithstanding, the analysis graph still shows a fast attenuation trend;

(c) When $\lambda_e < 0.10$, there is the problem of car body instability in the range of speed (160–200) km/h. It can be demonstrated that the motion is associated with the complex constrained singularity formed by the antirolling torsion bar devices, i.e., when the antirolling torsion bar devices are in-active or removed, the graphs of motor vehicle stability properties and variation patterns show that, as seen in Figure 3(e), the car body rolling mode tends to a self-stable state, and there is no problem of car body instability at this time.

However, since the HSR practices are often serviced on elevated lines with cross-wind or side-wind disturbances, the antirolling torsion bar devices cannot be removed or canceled. Therefore, the self-adaptive improved design should deal with the problem of car body instability at the minimum cost, and thoroughly solve and eliminate the car body shaking phenomenon and associated negative influences.

4. Semiactive Damping Validation Based on Three-Vehicle Trainset

Different from the troublesomeness of the primary hunting phenomenon, as shown in Figure 4, the self-adaptive improved design can decrease considerably the impact of car body instability on ride comfort merely by applying the semiactive damping technique between intervehicles, to solve car body instability when $\lambda_e < 0.10$ and $v = (160–200)$ km/h.

According to the preresearch and analysis based on a single vehicle, the dynamic simulation analyses of the MC01-TC02-MC03 three-vehicle trainset are composed of semiactive damping techniques of the intervehicles to change the car body rolling response into a Z-shaped car body yaw sway. As the inertia moment of car body yaw is much greater than that of car body rolling, $I_{zz} >> I_{xx}$, the self-adaptive improved design of high-speed bogies has handled the car body instability problem at the least cost.

When $\lambda_e \leq 0.10$ and within the speed range of (80–260) km/h, the beneficial influences of semiactive damping techniques on the ride comfort of the three-vehicle trainset have been fully verified under the following three tangent operation simulation conditions: (i) in the speed range of (80–140) km/h, the fifth-grade American track spectrum (AAR5) is used as the track irregularity excitation input; (ii) in the speed range of (160–200) km/h, the German track spectrum of high interference is used as the track irregularity excitation input; (iii) in the speed range of (220–260) km/h, the British small defect spectrum is used as the track irregularity excitation input.

5. Adaptability to Servicing Track Lines

Improving the adaptability to the servicing track line is one of the main objectives of the self-adaptive improved design of higher-/high-speed bogies, and it is also a necessary technical condition to realize the uniform wear strategy at

low conicity. As mentioned above, uniform wear at low conicity is one of the common goals in worldwide HSR practices. Despite long-term efforts, worldwide practices for improving the wheel-rail relationship have not yet achieved the technical goal. For German ICE rails, e.g., the values of track conicity with 50%, 95%, and 99% occurrence probability are 0.10, 0.20, and 0.30, respectively.

Under the configuration of novel antihunting dampers, the dynamic simulation analysis of a three-vehicle trainset can prove that the self-adaptive high-speed bogie has the ability to achieve this goal, thus forming our own key technology to control the instability hunting oscillation. To this end, this section fully verifies the adaptability of self-adaptive improved design to the servicing track lines under the following four conditions: variable gauge, variable track conicity, curving negotiation, and starting/braking in tangent lines.

5.1. Variable Gauge Condition. When running at 200 km/h in a tangent line, a track length of 5000 m, LM tread is selected for wheels, the lateral span between nominal rolling circles is 1493 mm, rail CN60KG with an inclination of 1/40, $\lambda_e = 0.10$. In the middle section of 500–1700 m, the gauge is increased by ca. 28.7 mm, the actual equivalent conicity λ_e is reduced from 0.10 to 0.03, and the front and the rear 100 m are transition sections, respectively.

Under the above variable gauge conditions, the technical effective comparison before and after the adaptation of the semiactive damping technique is shown in Figure 5. The semiactive damping technique between intervehicles effectively suppresses the strong vibration of car body rolling motion, as seen in Figure 5(b), and when λ_e is reduced from 0.10 to 0.03, the instability hunting oscillation becomes the hunting motion stabilization, and the low wear area spreading thereby, seen in Figures 5(c) and 5(d). The greater the wheel-rail clearance on each side, the stronger the response of the car body roll and rock is. However, the semiactive damping technique between intervehicles can effectively attenuate the above vibration responses.

5.2. Variable Track Conicity Condition. With the standard gauge $G = 1435$ mm, the three-vehicle trainset is running at 200 km/h in the tangent line same as above. However, the S1002 tread is used for the wheel, the lateral span between nominal rolling circles is 1500 mm, matching UIC rail E1 with an inclination of 1/32, and then $\lambda_e = 0.10$. In the middle distance of 1000 m, the rail inclination is changed to 1/27, and then $\lambda_e = 0.03$, and the front and the rear 100 m are transition sections, respectively.

Under the above variable track conicity conditions, the comparison of technical effectiveness before and after the adaption of the semiactive damping technique can be seen in Figure 6. Since the initial contact point on the rail is close to the centerline of the railhead, as shown in Figures 6(c) and 6(d), the increase in rail inclination from 1/32 to 1/27 has no obvious influence on the distribution characteristics of the wheel wear index. That is why Sweden rails are changed with the inclination of 1/30, and the gravity stiffness of the wheelset is then increased, which becomes one of the positive factors to promote the stability performance of X2000 or SJ3000 bogies.

From the above two contrastive analyses, the following three remarks can be achieved:

(a) When the lateral span between nominal rolling circles, $L = 1493$ mm at $\lambda_e = 0.10$, the wheel-rail clearance on each side increases by 3.5 mm compared with $L = 1500$ mm. However, the amplitude of the instability hunting oscillation cannot be increased considerably. More than that, since the wheel spin occurs, the distribution of the wheel wear index shows the characteristics of cocked up at both ends for the LM tread. Therefore, the correlation will be constituted between the lateral uneven power dissipation on the tread and the wheel profile updating design [41]. The narrower the low wear area is, the more serious the problem of lateral uneven power consumption on the tread is.

(b) Considering that the back-to-back distance of the wheelset is reduced to 1353 mm, the dynamical simulation analyses can prove that: $\lambda_e < 0.10$ is the rational condition of wheel-rail matching for Chinese HSR practices, and the low wear area becomes wider, by which the uniform wear stage can be formed at lower track conicity. Therefore, this high-quality technology resource of wheel-rail matching cannot be easily abandoned, which is one of the main objectives of the self-adaptive improvements.

(c) According to the momentum conservation law and $I_{zz} >> I_{xx}$, the semiactive damping technique can effectively improve ride comfort. And the conclusion of linear stability analysis is fully verified under variable gauge conditions, i.e., there is a correlation between the simple car body instability and the complex constraint singularity change of antirolling torsion bar devices.

5.3. Curve Negotiation and Starting/Braking Condition. Similarly, taking the curving negotiation of a three-vehicle trainset as an example, as shown in Figure 7, LMA tread is selected for wheels, the lateral span of nominal rolling circles is 1493 mm, the rail CN60KG with an inclination of 1/40, $\lambda_e = 0.03$, the radius of the circular curve is 3000 m, the superelevation of the outer rail is 100 mm, and the equilibrium speed is 160 km/h.

Under the semiactive damping technique between intervehicles, the unstable movement of the car body is greatly suppressed, and the $(\mathrm{RMS})_{3\sigma}$ of lateral track-shift force is far less than the safety threshold of ca. 25 kN. The tread wear is partially converted into flange wear. If the actual routing is planned reasonably, the equilibrium between tread wear and flange wear can be achieved thereby, and the necessary technical guarantee for realizing economic reprofiling can be provided by applying the self-adaptive improved design.

For the same reason, make the starting/braking process more stable. Take the starting of the three-vehicle trainset in

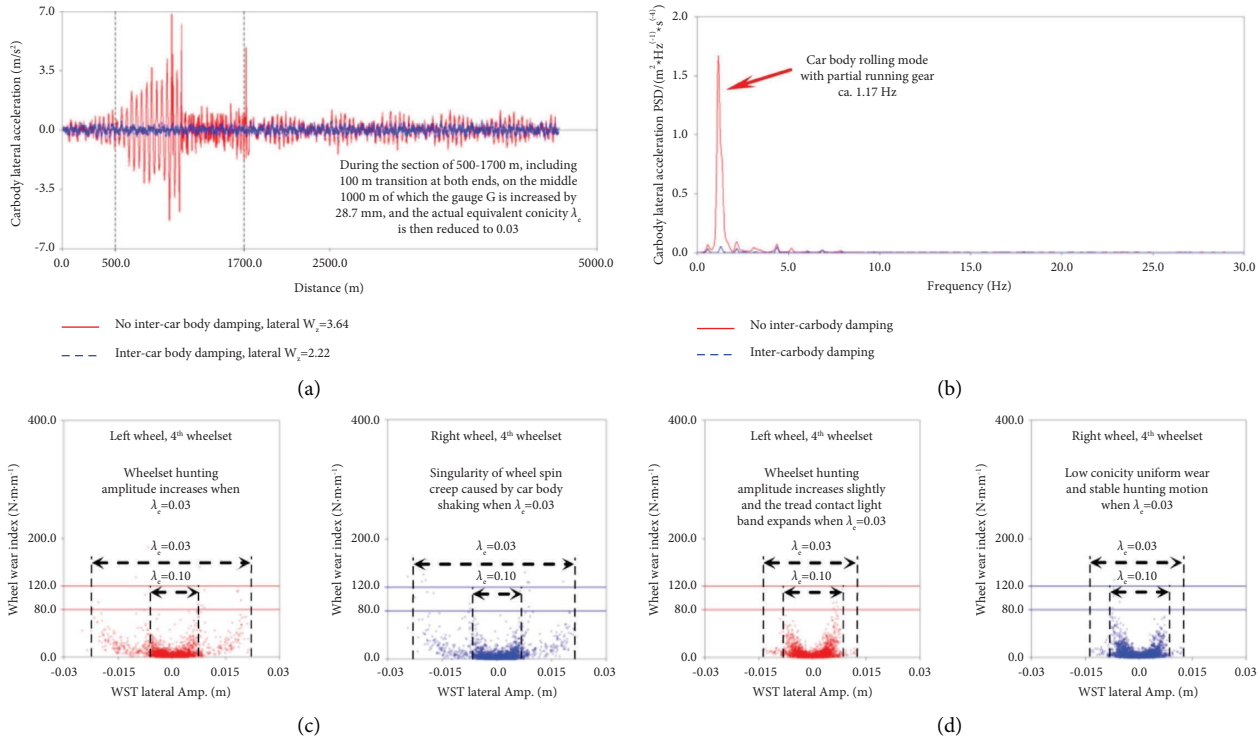

Figure 5: Effective assessments of the semiactive damping technique at MC03 under variable gauge conditions. (a) Lateral acceleration contrast at the rear-right point on the car body floor. (b) Lateral acceleration PSD contrast at the rear-right point on the car body floor. (c) Distribution contrast of wheel wear index characteristics when intervehicle damping off. (d) Distribution contrast of wheel wear index characteristics when intervehicle damping is on.

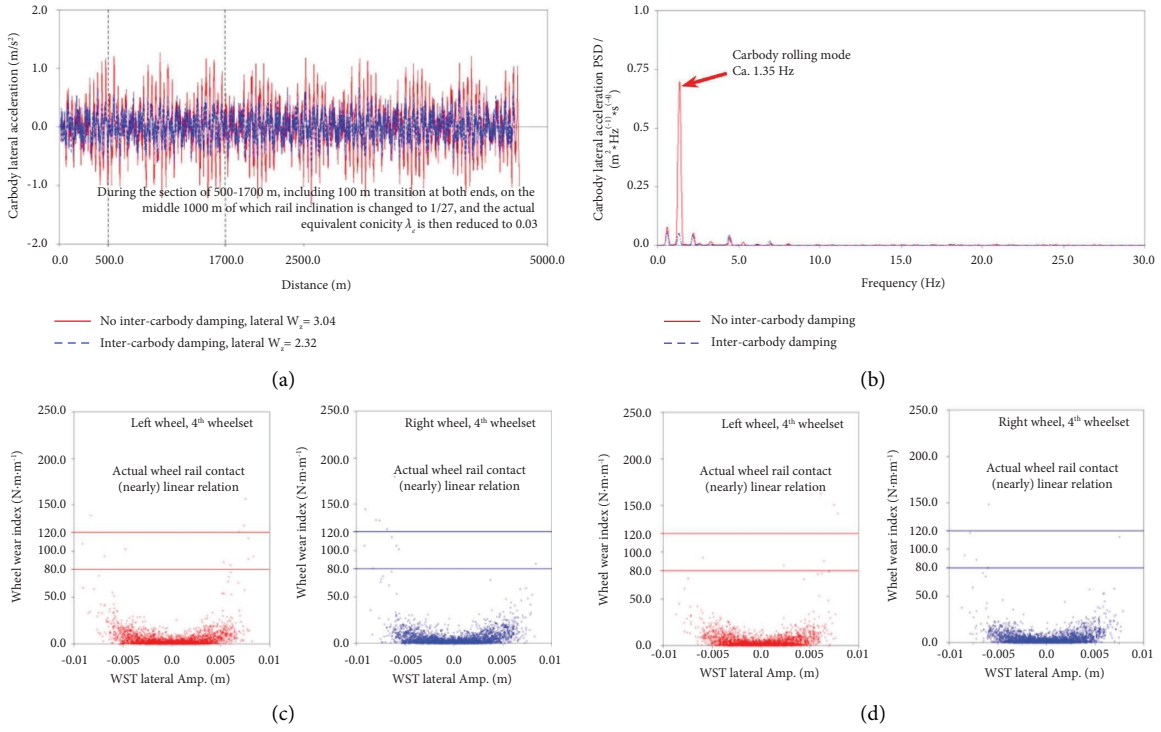

Figure 6: Effective assessments of the semiactive damping technique at MC03 under variable track conicity conditions. (a) Lateral acceleration contrast at the rear-right point on the car body floor. (b) Lateral acceleration PSD contrast at the rear-right point on the car body floor. (c) Distribution contrast of wheel wear index characteristics when intervehicle damping is off. (d) Distribution contrast of wheel wear index characteristics when intervehicle damping is on.

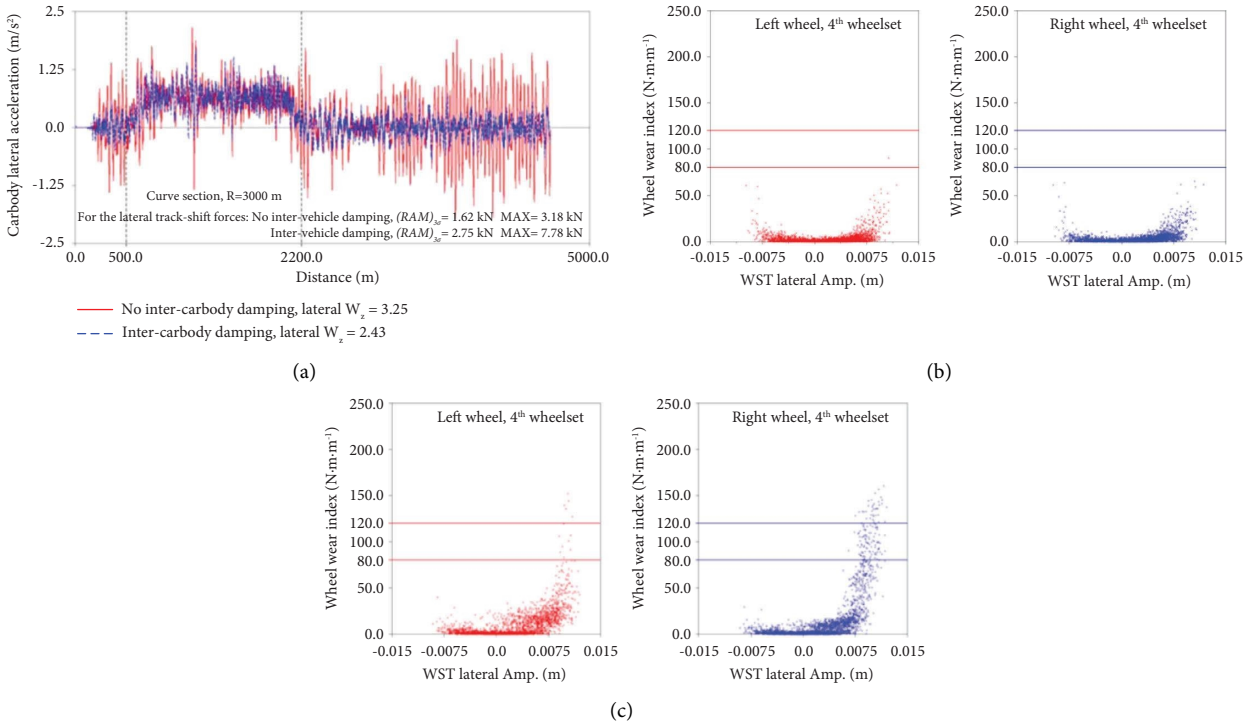

Figure 7: Effective assessments of MC03 under a curving negotiation condition of R3000 m/superelevation 100 mm and a velocity of 160 km/h. (a) Lateral acceleration contrast at the rear-right point on the car body floor. (b) Distribution contrast of wheel wear index characteristics when intervehicle damping is off. (c) Distribution contrast of wheel wear index characteristics when intervehicle damping is on.

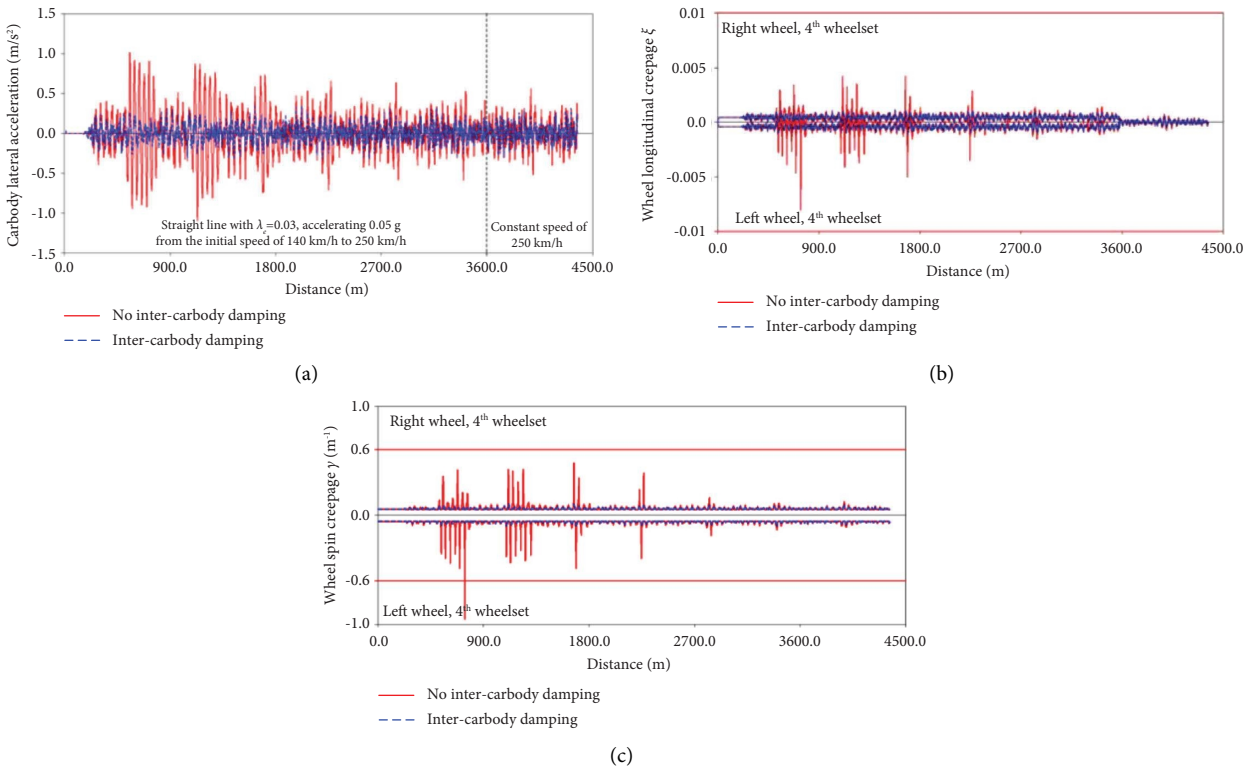

Figure 8: Effective assessments of MC03 under starting/braking conditions. (a) Lateral acceleration contrast at the rear-right point on the car body floor. (b) Wheel longitudinal creepage ξ. (c) Wheel spin creepage γ.

a tangent line with $\lambda_e = 0.03$ as an example, as shown in Figure 8, accelerating 0.05 g from the initial speed of 140 km/h to 250 km/h, the effectiveness of the semiactive damping technique is very beneficial.

The wheel creepage is stable under the semiactive damping technique between intervehicles, e.g., longitudinal creepage ($\xi < 0.01$) and spin creepage ($\gamma < 0.6$). Therefore, the self-adaptive improved design is fully capable of ensuring a smooth starting and acceleration process under bad weather conditions with a reduced traction coefficient, and avoiding the flat scar wheel or (shallow-) surface cracks as much as possible.

The self-adaptive improved design of higher-speed bogies can be demonstrated similarly with the parallel configuration of ZF Sachs T60 and T70 dampers, which has the ability to explore the dynamic behavior laws of higher speeds.

The realization mode of a semiactive damping technique between intervehicles should fully learn from the vehicle-end vibration reduction of one of the Japanese Shinkansen trains to attenuate the car body upswing vibrations. Monobar traction devices and no antirolling torsion bar devices are two of the outstanding technical features of Japanese Shinkansen bogies. In order to attenuate the upswing vibration of the service car body, the vehicle-end vibration reduction device consists of two dampers with dual rotating arms and one connecting rod. The dampers installed, respectively, on the end walls of the front and rear car bodies are hinged with the connecting rod through the dual rotating arms. When the relative distance or yaw is changed between intervehicles, the two dampers can dissipate the kinetic energy of the service car body upswing through the dual rotating arms. At the same time, use the springs to reset the dampers as soon as possible.

As mentioned above, the self-adaptive improved design of higher-/high-speed bogies should achieve the following three important goals at the lowest cost: firstly, formulate the uniform wear strategy at low conicity; secondly, promote the self-cleaning ability of detrimental wear; and thirdly, scientifically explore the higher-speed dynamic behavior laws in order to optimize the repair class and repair system. Therefore, we must attach importance to the preconditions for the application of present techniques or software, i.e., the dynamic design methodology is actively introduced in Chinese HSR practices, clarifying the self-adaptive improved direction as soon as possible by using the proper orthogonal decomposition approach and modal modification response technique.

6. Conclusions and Prospects

In postindustrial society, as a typical research case of large-scale complex nonlinear systems, HSRS have two classic nonlinearities such as nonsmooth and large displacement. Consequently, the re-innovation of associated imported technologies must be combined with the particularities of Chinese HSR practices. In view of the design default of the primary hunting phenomenon that existed in the prototype of German ICE3 serial bogies, the HSRS dynamic design methodology was proposed in the preliminary research, in which the analysis graphs of full-vehicle stability properties and variation patterns have clarified the correct direction of self-adaptive improvements. On this basis, this paper further solves the service car body instability problem at the minimum cost and realizes the technical goal of scientifically promoting the limit and construction speeds under the rational conditions of wheel-rail matching.

Through the above research works, the following three main conclusions can be drawn:

(a) Since the back-to-back distance of the wheelset is shortened to 1353 mm, $\lambda_e < 0.10$ is the rational matching condition for Chinese HSR practices. The low-wear area becomes then wider, which can enhance the adaptability of HSRS to different speed-grade dedicated lines and their service conditions. The improved design of the wheel-rail relationship should not simply give up this high-quality technical resource of low-track conicity just because of the primary hunting default that existed in the prototype design of German ICE3 serial bogies. Therefore, this research proposes that only the self-adaptive improved designs for higher-/high-speed bogies can solve the difficult problem of the primary hunting phenomenon at the least technical cost. Then, under the rational condition of wheel-rail matching, the difficult problem of detrimental wear can be overcome through the collaborative innovation efforts of multiple disciplines.

(b) On the premise of meeting the requirements of crossing over different speed grades of dedicated lines, the dynamic analyses can demonstrate that only the semiactive damping technique between intervehicles is necessary to be adapted so as to realize the running operations on the three-speed levels of 160/250/350 km/h. For the self-adaptive improved design of higher-/high-speed bogies, the economic reprofiling requirements of wheelsets can conditionally be satisfied through optimal routing planning.

(c) In order to meet the dynamic gauge requirements, the antirolling torsion bar device is one of the necessary configurations for HSRS, but the associated singularity changes of complex constraints constitute a correlation relationship with the simple car body instability problem investigated in this paper, i.e., the self-excited resonance of car body rolling motion or car body upswing oscillation. The semiactive damping technique cleverly changes the car body rolling into a Z-shaped yaw motion, and uses $I_{zz} >> I_{xx}$ to improve the impact on ride comfort, thus creating favorable technical conditions for realizing the uniform wear strategy at low conicity. So the self-adaptive improved design of higher-/high-speed bogies has achieved the technical goal of solving the primary hunting problem at the minimum cost.

Different from the improved design of the HSR wheel-rail relationship, the self-adaptive improved design of

higher-/high-speed bogies regresses to the rational condition of wheel-rail matching at the minimum cost. Then, through MDO, the following three important goals will be achieved: formulating the uniform wear strategy at low conicity, promoting the self-cleaning ability for detrimental wear, and exploring a higher speed dynamic behavior law to optimize the repair class and repair system.

Data Availability

The datasets generated during and/or analyzed during the current study are available from the corresponding author on reasonable request.

Conflicts of Interest

The authors declare that they have no conflicts of interest.

Acknowledgments

The authors would like to thank the on-site staff for providing relevant data support. This work was supported by the National Key R&D Program of China (Grant nos. 2018YFB1201703, 2017YFB0304605, and 2020YFB1200200ZL) and the Research Project of National Innovation Center of High Speed Train (Grant no. CXKY-02-01-02(2020)).

References

[1] J. Raczynski, *Trans-European Railway High-Speed MASTER PLAN STUDY PHASE 2-A General Background to Support Further Required Studies*, Unided Nations Publication, New York, NY, USA, 2021.

[2] T. Matsudaira, "Paper 7: hunting problem of high-speed railway vehicles with special reference to bogie design for the new tokaido line," *Proceedings of the Institution of Mechanical Engineers, Conference Proceedings*, vol. 180, no. 6, pp. 58–66, 1965.

[3] A. H. Wickens, *Fundamentals of Rail Vehicle Dynamics: Guidance and Stability*, Swets & Zeitlinger Publishers, Lisse, Netherlands, 2005.

[4] K. Knothe and S. Stichel, *Rail Vehicle Dynamics*, Springer, Berlin, Germany, 2017.

[5] S. Z. Meymand, A. Keylin, and M. Ahmadian, "A survey of wheel–rail contact models for rail vehicles," *Vehicle System Dynamics*, vol. 54, no. 3, pp. 386–428, 2016.

[6] W. Schiehlen, "On the history of lateral ground vehicle motions from a multibody dynamics view," *Journal of Computational and Nonlinear Dynamics*, vol. 10, no. 3, Article ID 031014, 2015.

[7] M. Zacher, D. Nicklisch, G. Grabner, O. Polach, and B. Eickhoff, "A multi-national survey of the contact geometry between wheels and rails," *Proceedings of the Institution of Mechanical Engineers - Part F: Journal of Rail and Rapid Transit*, vol. 229, no. 6, pp. 691–709, 2015.

[8] F. Gan, H. Y. Dai, H. Gao, and M. R. Chi, "Wheel-rail contact relationship of worn LMA tread," in *Proceedings of the 2013 23rd IAVSD Symposium*, Qingdao, China, August 2013.

[9] T. Tomioka, T. Takigami, A. Fukuyama, and T. Suzuki, "Prevention of carbody vibration of railway vehicles induced by imbalanced wheelsets with displacement-dependent rubber bush," *Journal of mechanical systems for transportation and logistics*, vol. 3, no. 1, pp. 131–142, 2010.

[10] V. Bokaeian, M. A. Rezvani, and R. Arcos, "Nonlinear impact of traction rod on the dynamics of a high-speed rail vehicle carbody," *Journal of Mechanical Science and Technology*, vol. 34, no. 12, pp. 4989–5003, 2020.

[11] M. R. Hou, X. Y. Hu, and H. T. Li, "Study on the longitudinal-vertical coupling vibration of high-speed vehicle based on newmark-β forecast-correction integral method," *China Railway Science*, vol. 39, no. 3, pp. 57–62, 2018.

[12] M. Sayed and M. Kamel, "1: 2 and 1: 3 internal resonance active absorber for non-linear vibrating system," *Applied Mathematical Modelling*, vol. 36, no. 1, pp. 310–332, 2012.

[13] D. Gong, K. Zhao, G. Liu, Z. Wang, T. You, and J. Zhou, "Modal vibration decomposition method and its application on multi-mode vibration control of high-speed railway car bodies," *Journal of the Franklin Institute*, vol. 359, no. 10, pp. 4699–4726, 2022.

[14] T. You, J. Zhou, D. J. Thompson, D. Gong, J. Chen, and Y. Sun, "Vibration reduction of a high-speed train floor using multiple dynamic vibration absorbers," *Vehicle System Dynamics*, vol. 60, no. 9, pp. 2919–2940, 2022.

[15] M. W. Piao, J. Yang, D. Z. Liu, J. Fang, and D. M. Tian, "Design defaults of German ICE3 serial bogies and technical solutions," *Computer Integrated Manufacturing Systems*, vol. 22, no. 7, pp. 1654–1669, 2016.

[16] X. Q. Dong, Y. M. Wang, Z. S. Ren, L. D. Wang, and H. Y. Liu, "Design and application of thin flange wheel tread profiles for CRH3C EMUs," *Journal of the China Railway Society*, vol. 36, no. 2, pp. 11–17, 2014.

[17] F. Gan, H. Dai, H. Gao, and M. Chi, "Wheel-rail wear progression of high speed train with type S1002CN wheel treads," *Wear*, vol. 328-329, pp. 569–581, 2015.

[18] O. Polach, "Wheel profile design for target conicity and wide tread wear spreading," *Wear*, vol. 271, no. 1-2, pp. 195–202, 2011.

[19] O. Polach and D. Nicklisch, "Wheel/rail contact geometry parameters in regard to vehicle behaviour and their alteration with wear," *Wear*, vol. 366-367, pp. 200–208, 2016.

[20] M. R. Hou, F. S. Liu, Z. Zhang, D. Cheng, and X. Fang, "Typical wheel-rail profile change and matching characteristics of high-speed railway in China," *China Railway Science*, vol. 41, no. 4, pp. 99–107, 2020.

[21] Y. Wu, J. Zeng, S. Qu, H. Shi, Q. Wang, and L. Wei, "Low-frequency carbody sway modelling based on low wheel-rail contact conicity analysis," *Shock and Vibration*, vol. 202017 pages, Article ID 6671049, 2020.

[22] J. Guo, H. Shi, F. Li, and P. Wu, "Field measurements of vibration on the carbody suspended equipment for high-speed rail vehicles," *Shock and Vibration*, vol. 202015 pages, Article ID 6041543, 2020.

[23] Z. H. Yang, H. Y. Dai, and J. J. Shi, "Analysis of worn wheel-rail contact relationship and line adaptability," *Journal of the China Railway Society*, vol. 43, no. 5, pp. 37–46, 2021.

[24] T. T. Li, Q. B. Wang, and M. W. Piao, "Wheelset self-stability and MBS simulations of speeding-up railway vehicles," *Journal of East China Jiaotong University*, vol. 38, no. 2, pp. 103–109, 2021.

[25] Q. Y. Zhou, F. S. Liu, Y. H. Zhang, C. Tian, Z. Yu, and J. Zhang, "Solutions for problems at wheel-rail interaction in high speed railway," *China Railway Science*, vol. 38, no. 5, pp. 78–84, 2017.

[26] Y. G. Ye and Y. Sun, "Reducing wheel wear from the perspective of rail track layout optimization," *Proceedings of the Institution of Mechanical Engineers - Part K: Journal of Multi-body Dynamics*, vol. 235, no. 2, pp. 217–234, 2021.

[27] T. T. Li, M. W. Piao, J. Fan, Z. Fang, S. Jin, and G. Li, "Dynamic design of self-adaptive high-speed bogies based on full-vehicle stability properties and variation patterns," *Computer Integrated Manufacturing Systems*, vol. 28, no. 2, pp. 385–408, 2022.

[28] T. T. Li, W. Du, M. W. Piao et al., "Dynamical effect investigations of component's internal interface by using techniques of rigid-flex coupling simulation," *Shock and Vibration*, vol. 2021, pp. 1–13, Article ID 6509950, 2021.

[29] S. Iwnicki, *Handbook of Railway Vehicle Dynamics*, CRC Press, Boca Raton, Fl, USA, 2006.

[30] H. True, A. P. Engsig-Karup, and D. Bigoni, "On the numerical and computational aspects of non-smoothnesses that occur in railway vehicle dynamics," *Mathematics and Computers in Simulation*, vol. 95, pp. 78–97, 2014.

[31] D. Negrut and J. L. Ortiz, "A practical approach for the linearization of the constrained multibody dynamics equations," *Journal of Computational and Nonlinear Dynamics*, vol. 1, no. 3, pp. 230–239, 2006.

[32] E. J. Haug, D. Negrut, and M. Lancu, "A state-space-based implicit integration algorithm for differential-algebraic equations of multibody dynamics," *Mechanics of Structures and Machines*, vol. 25, no. 3, pp. 311–334, 1997.

[33] D. Dopico, F. González, J. Cuadrado, and J. Kovecses, "Determination of holonomic and nonholonomic constraint reactions in an index-3 augmented Lagrangian formulation with velocity and acceleration projections," *Journal of Computational and Nonlinear Dynamics*, vol. 9, no. 4, Article ID 041006, 2014.

[34] J. T. Allison and D. R. Herber, "Special section on multidisciplinary design optimization: multidisciplinary design optimization of dynamic engineering systems," *AIAA Journal*, vol. 52, no. 4, pp. 691–710, 2014.

[35] S. Hiwa, T. Hiroyasu, and M. Miki, "Design mode analysis of Pareto solution set for decision-making support," *Journal of Applied Mathematics*, vol. 201415 pages, Article ID 520209, 2014.

[36] A. Oyama, K. Fujii, K. Shimoyama, and M. S. Liou, "Pareto-optimality-based constraint-handling technique and its application to compressor design," in *Proceedings of the 17th AIAA Computational Fluid Dynamics Conference*, Toronto, Ontario, Canada, 2005 June.

[37] M. Krack, L. Panning-von Scheidt, and J. Wallaschek, "A method for nonlinear modal analysis and synthesis: application to harmonically forced and self-excited mechanical systems," *Journal of Sound and Vibration*, vol. 332, no. 25, pp. 6798–6814, 2013.

[38] T. Marinone, P. Avitabile, J. Foley, and J. Wolfson, "Efficient computational nonlinear dynamic analysis using modal modification response technique," *Mechanical Systems and Signal Processing*, vol. 31, pp. 67–93, 2012.

[39] Z. G. Fang, C. Guo, M. W. Piao, G. D. Li, and J. Fan, "Investigations on detrimental wear formation mechanism of high-speed rails and feedback negative impacts," *Journal of Dalian Jiaotong University*, vol. 41, no. 6, pp. 51–56, 2020.

[40] M. W. Piao, C. Guo, W. Du, G. D. Li, and J. Fan, "Influences of anti-rolling torsion-bar fixed/floated simple supports to formations of detrimental worn treads," *Journal of Dalian Jiaotong University*, vol. 42, no. 5, pp. 59–65, 2021.

[41] G. I. Alarcón, N. Burgelman, J. M. Meza, A. Toro, and Z. Li, "Power dissipation modeling in wheel/rail contact: effect of friction coefficient and profile quality," *Wear*, vol. 366-367, pp. 217–224, 2016.

[42] C. Qu, Y. Li, J. Z. Jiang et al., "Reducing wheel–rail surface damage by incorporating hydraulic damping in the Bogie primary suspension," *Vehicle System Dynamics*, 2022.